

Triclinic α -LiVOPO₄/C High-performance Cathode material synthesized via a ball-milling method

Jingjing Cai¹, Zhi Su^{1,2,*}, Weigang, Fan^{1,2}

¹ College of Chemistry and Chemical Engineering, Xinjiang Normal University, Urumqi, 830054, Xinjiang, China

² Xinjiang Key Laboratory of Energy Storage and Photoelectrocatalytic Materials, Urumqi, 830054, Xinjiang, China

*E-mail: suzhixj@sina.com

Received: 2 October 2020 / Accepted: 29 November 2020 / Published: 31 December 2020

Triclinic Lithium vanadyl phosphate (α -LiVOPO₄) as a cathode material for Lithium ion batteries was prepared via a route of mechanical ball-milling method. Using carbon material (acetylene black) as the carbon source, V₂O₅, NH₄H₂PO₄, CH₃COOLi and oxalic acid as raw materials to synthesis the α -LiVOPO₄/C. And the morphology of the sample was analyzed by TEM. The result of TEM shows that the surface of α -LiVOPO₄/C has a layer of carbon (3.6 nm), this is due to acetylene black formed a layer of carbon on the surface of α -LiVOPO₄ particles after thermal decomposition. Its existence effectively alleviated the agglomeration phenomenon of materials under high temperature calcination, increasing the conductive area of the material, reducing the polarization of the battery during charging and discharging process, and improved the electrochemical property of α -LiVOPO₄. In addition, the material could provide an initial capacity of 157.4 mAh g⁻¹ at 0.05 C (sintered at 600 °C). And it also could provide a discharge capacity of 155.6 mAh·g⁻¹ by the 50th cycle, the capacity retention rate was 98.8%.

Keywords: electrochemical properties; α -LiVOPO₄/C; acetylene black

1. INTRODUCTION

Due to the advantages of environmental protection, safety, convenient transportation, low cost and large capacity, Lithium-ion battery plays an significant status in the energy and chemistry sector. Since the olivine structured LiFePO₄ [1-3] was commercialized in 1997, there have been studies on polyanionic phosphate materials, like LiM₁PO₄ (M₁=Co, Mn, Ni) [4-7], Li₃M₂PO₄ (M₂= V, Fe, Cr) [8-11], LiTi₂(PO₄)₃ [12-13] etc. are promising; but they have some common faults like poor cycle stability, high cost, and low-voltage platform. In order to meet people's demand for high energy

density batteries, it is urgent to research a high energy density, low cost and high voltage cathode material for lithium ion batteries.

The theoretical capacity of LiVOPO_4 [14–16] is 159 mAh g^{-1} , it is lower than LiFePO_4 (170 mAh g^{-1}) a bit, but LiVOPO_4 provides a higher voltage platform (3.9 V) and higher energy density (616 Wh kg^{-1}) than LiFePO_4 (3.6 V, 578 Wh kg^{-1}). LiVOPO_4 is a polymorph, which have α_1 -, β -, ϵ - and α - LiVOPO_4 , they have been reported by different methods. Among them, the α_1 phase (tetragonal, $P4/nmm$) of LiVOPO_4 [17-20] exhibiting 2D Li diffusion with a layer structure, and because it is difficult to synthesize, it has been less reported. The β phase (orthorhombic, $Pnma$) of LiVOPO_4 [21-23] exhibiting 1D Li diffusion and the ϵ phase (triclinic, $P\bar{1}$) of LiVOPO_4 [24-25] has pseudo-1D diffusion. The β and ϵ phases can be synthesized through many methods, like solid-state [26] hydrothermal [27] and sol-gel [28].

In this paper, we will study the preparation of α - LiVOPO_4 . After α - LiVOPO_4 was calcined in the air, and a small amount of carbon remained on its surface, oxalic acid as carbon source was not enough to improve its ionic conductivity. This paper provided a route to obtain α - LiVOPO_4 sample with uniform material particles. Acetylene black was added as carbon coating material in the preparation process of the precursor, and the carbon produced by acetylene black cracking at high temperature could coat the outer surface for the material, thus improving its electrical conductivity. The electrochemical property of LiVOPO_4/C was improved in comparison to previously reported one [29]. As expected, α - LiVOPO_4/C material was synthesized and its electrochemical behavior implies that it has a widely potential application.

2. EXPERIMENTAL

2.1 Sample preparation

The precursor of α - LiVOPO_4 was prepared using CH_3COOLi (AR, $\geq 99.0\%$), V_2O_5 (AR, $\geq 98.0\%$) and $\text{NH}_4\text{H}_2\text{PO}_4$ (AR, $\geq 99.0\%$), oxalic acid (AR, $\geq 98.0\%$). First, all reagents were stirred evenly with 20 g agate beads in a ball milling tank for six hours (deionized water as solvent). Then the solution was dried at 140°C , and sample sintered at 400°C for four hours in air atmosphere and cooled to room temperature. Second, acetylene black (mass fraction 10%), precursor and deionized water of 20 ml in a planetary ball mill uniform mixed for six hours, subsequently, dried the mixture at 60°C to obtain the sample. Finally, the sample was calcined under three temperatures for ten hours in a tubular furnace to get the α - LiVOPO_4/C power.

2.2 Characterization

Phase identification of the α - LiVOPO_4/C were detected by X-ray diffraction (Bruker D2 Cu α (λ : 1.5418) 30 Kv, radiation: 10° – 70° , step size: 0.02°). The micro-structure result was obtained by TEM (FEI Tecnai G2 F20) .

First, the electrode slurry was prepared by mixing α - LiVOPO_4/C power and Polyvinylidene fluoride (PVDF) with the ratio of 1:1 (deionized water as solvent), the mixture slurry was then daubed

on Al foil uniformly and dried at 110 °C. Next, cutting the Al foil into electrodes with an area of 1.2 cm², using compose of 1.0M LiPF₆ with the ratio of EC:DMC:DEC=1:1:1 Vol% and 1.0%VC (LB-266) as the electrolyte, using Lithium metal as a counter electrode. Finally, button cells were assembled in a Braun vacuum glove box with Ar-filled. After setting 24 h, batteries were used for electrochemical performance tests.

The charge/discharge test was carried out by LAND Test System (CT2001A, Wuhan), the CV test was carried out by the electrochemical workstation (CHI650D, Shanghai Chenhua) at room temperature in the voltage range of 3–4.5 V, and the AC impedance test was carried out in the amplitude of 5 mV, frequency range of 1 mHz–1 MHz.

3. RESULTS AND DISCUSSION

3.1. Structure and morphology

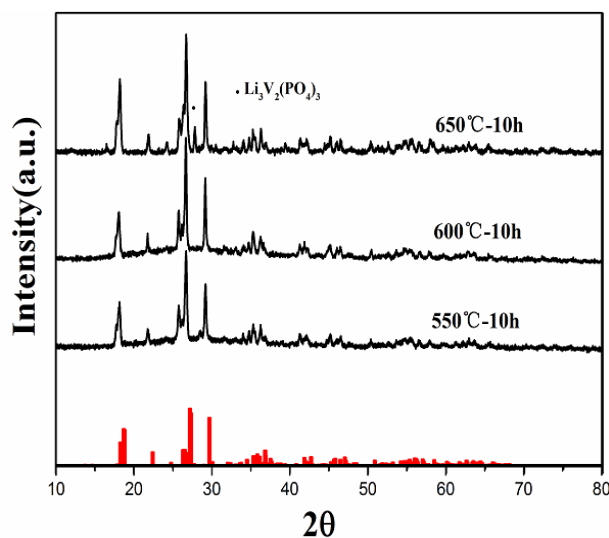


Figure 1. XRD diagram of α -LiVOPO₄/C sintered at at different temperatures

The XRD pattern of the α -LiVOPO₄/C prepared at different temperatures is present in Fig.1. It can be seen that the peaks type are correspond with the phase of α -LiVOPO₄ (PDF # 72-2253) at 550 °C and 600 °C and without impurity diffraction peak, it shows that α -LiVOPO₄/C were prepared successfully under this two different temperatures. Meanwhile, the diffraction peak of carbon could not be seen in the X-ray diffraction pattern. Which indicates that acetylene black was successfully coated the outer surface of the material. The result shows that the carbon coating did not change the structure of the α -LiVOPO₄. With the increase of temperature, the crystallinity of material became better and better. But, when calcination temperature was upped to 650 °C, appears a peak of Li₃V₂(PO₄)₃ at 28.10°(2 θ) [30], this might be caused by the too high calcination temperature lead to the production of other substances.

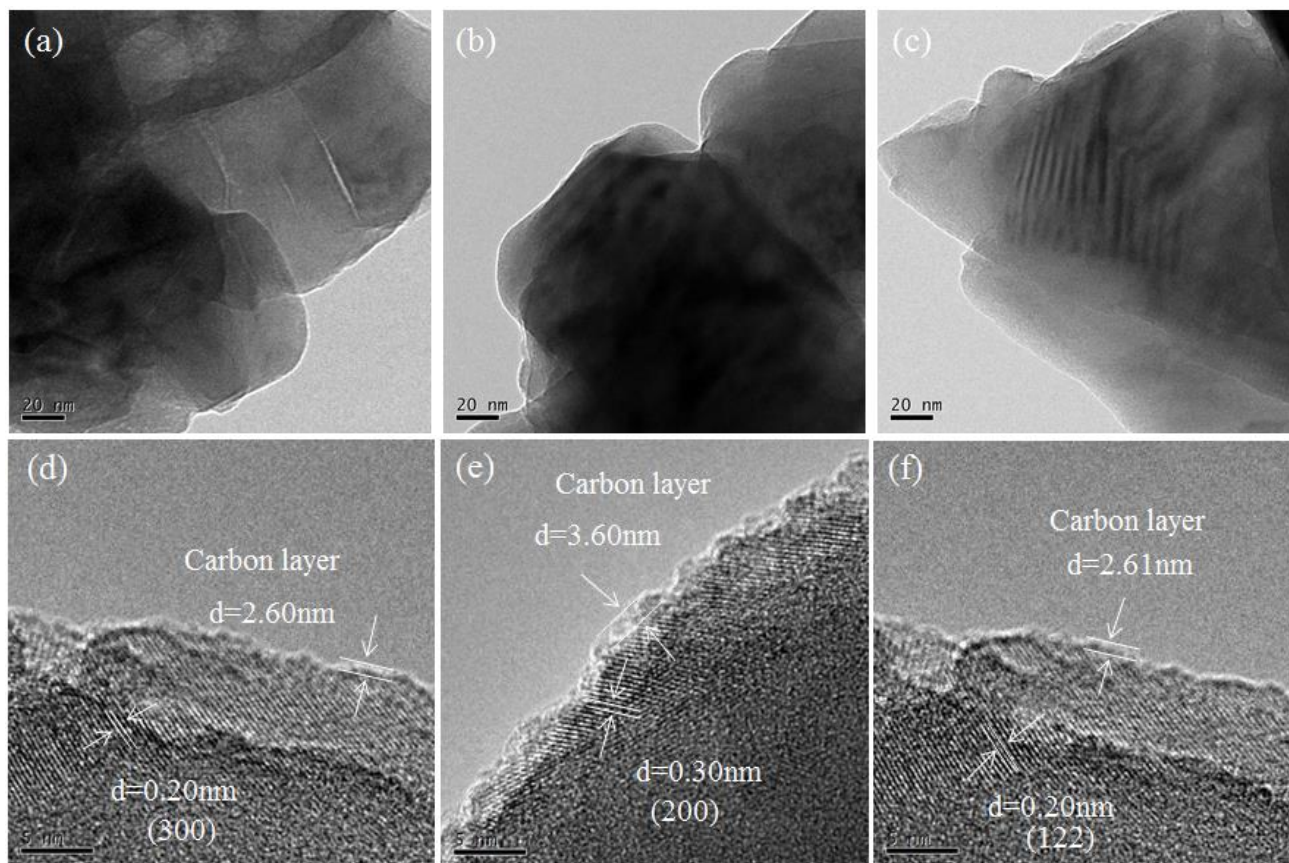


Figure 2. (a) - (f) TEM diagrams of α -LiVOPO₄/C sintered at different temperature

TEM images of sintered materials at different temperatures are shown in Figure 2. It can be seen from Fig. (2a) (2b) (2c) that after calcination (550°C, 600°C, 650°C), the morphology of α -LiVOPO₄/C materials showed irregular shape and the size of the material were about 20-100 nm. Fig. (2d) (2e) (2f) showed that the carbon layer [31] $d=2.60$ nm, $d=3.60$ nm, $d=2.61$ nm (at 550°C, 600°C, 650°C) produced by acetylene black pyrolysis inhibited the continuous increase of grain size under high temperature calcination, and had a good regulating effect on the preparation of nanoscale material. In addition, marking lattice spacing $d=0.20$ nm, $d=0.30$ nm, $d=0.21$ nm (at 550°C, 600°C, 650°C) and corresponds to the (300) crystal plane, (200) crystal plane, (121) crystal plane.

3.2. Electrochemical performance

As can be seen from the figure, the charging and discharging platform of α -LiVOPO₄/C is about 3.9 V. In Fig. 3, the α -LiVOPO₄/C could provide an initial discharge capacity of 150 mAh g⁻¹ (sintered at 550 °C). And with the crystallinity of the materials tended to be better when the synthesis temperature increased, the initial capacity of the material prepared at 600 °C was higher than 550 °C, which increased to 157.4 mAh g⁻¹. But when the synthesis temperature increased to 650 °C, the material provided a lower initial capacity (152.5 mAh g⁻¹) than 600 °C (157.4 mAh g⁻¹). This might be the sintering temperature of the material at 650 °C was higher, the agglomeration between material

particles occurred, and the insertion and emigration distance of Li^+ in crystal structure increases, this allowed only a few Li^+ to move back and forth per unit time. As a result, the initial capacity of material prepared at 600°C was superior to 650°C . Moreover, the charge and discharge plateau of materials were similar with the reports of literatures [29,32,33], but the discharge capacitance was higher than the reported of Liu et al. [29], and it's closer to theoretical capacity. The reason might be that the two-step ball milling method made the obtained material had a smaller particle size. The comparison with similar cathode materials for LIBs are shown in Table 1.

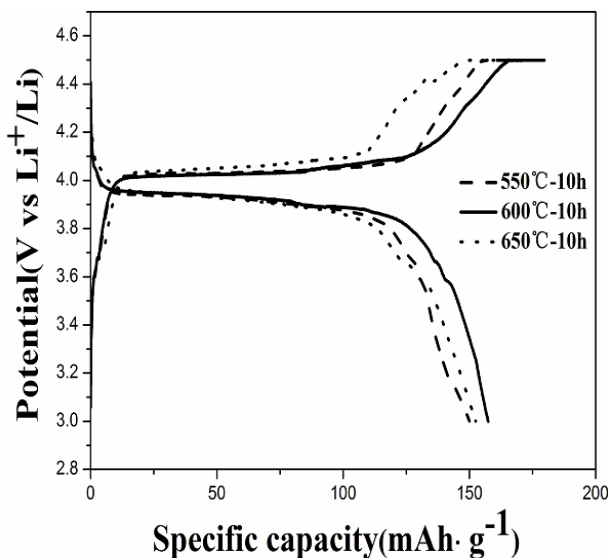


Figure 3. First cycle charge/discharge curves of $\alpha\text{-LiVOPO}_4/\text{C}$ sintered at three different temperatures, and with the voltage range of 3–4.5 V, at 0.05 C.

Table 1. Comparison with similar cathode materials for LIBs

Cathode materials	Voltage platform (V)	Theoretical capacity (mAh g^{-1})	Energy density (Wh kg^{-1})	Refs.
LiCoPO_4	4.8	167	800	[39]
LiMnPO_4	4.1	170	701	[38]
LiNiPO_4	5.1	170	867	[37]
LiFePO_4	3.6	170	578	[29]
$\text{Li}_3\text{V}_2(\text{PO}_4)_3$	4.3	132	500	[40]
LiVOPO_4	3.9	159	616	[29]
LiVOPO_4 (550°C)	3.9	150	585	This work
LiVOPO_4 (600°C)	3.9	157.4	614	This work
LiVOPO_4 (600°C)	3.9	152.5	595	This work

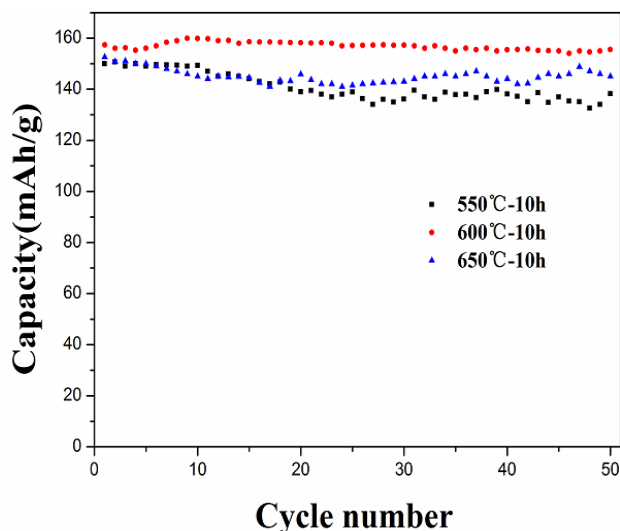


Figure 4. Cycle life diagrams of α -LiVOPO₄/C sintered at three different temperatures and with the voltage range of 3–4.5 V, at 0.05 C.

From the figure, we can see that the capacity retention rate of materials prepared at 600 °C was best (98.8%), the material still could provide a capacity of 155.6 mAh·g⁻¹ by the 50th cycle. The average weekly capacity loss rate of material was only 0.036%. At the same time, the materials synthesized at 550 °C and 650 °C could provide the capacity of 138.2 mAh·g⁻¹ and 145 mAh·g⁻¹ respectively, after 50 cycles. The results (retention rates of capacity after 50 cycles) of the materials prepared at 550 °C, 600 °C, 650 °C were consistent with the initial discharge capacity. It also shows that the addition of acetylene black improved the electrochemical performance of the α -LiVOPO₄. This might be the α -LiVOPO₄ was coated with amorphous carbon, the presence of carbon prevented the side reaction occurs between electrolyte and material, and the electrochemical impedance between electrode surface and electrolyte interface was reduced. In addition, the carbon could improve the material conductivity and reduce the battery polarizability.

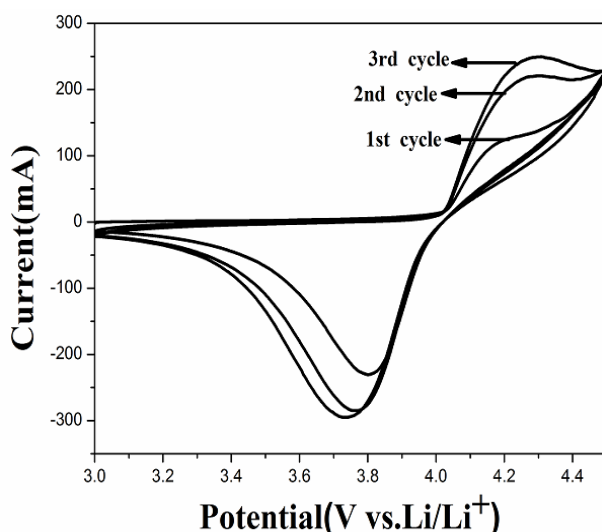


Figure 5. Cyclic Voltammetry of α -LiVOPO₄/C sintered at 600 °C; with the voltage range of 3–4.5 V, with the sweep speed of 0.1 mV/s.

In order to know the cyclic reversibility of material synthesized at 600 °C, cyclic voltammetry was tested with the material. The oxidation peaks and reduction peaks are seen clearly from the picture, which shows the α -LiVOPO₄/C only corresponds to the process of Li⁺ free de-intercalation [34]. In terms of the 3rd cycle, its oxidation peak and reduction peak are 4.22V and 3.73V respectively, a large difference indicates a large degree of polarization of the material. The reason may be the effect of conductive agent on material; and the low conductivity of electrolyte. The symmetry of oxidation peaks and reduction peaks indicate that the electrode reaction was reversible. In addition, the degree of curve coincidence in the first three cycles are low, indicating that certain polarization phenomenon occurs in the charging and discharging process of the material, which leads to the occurrence of irreversible changes.

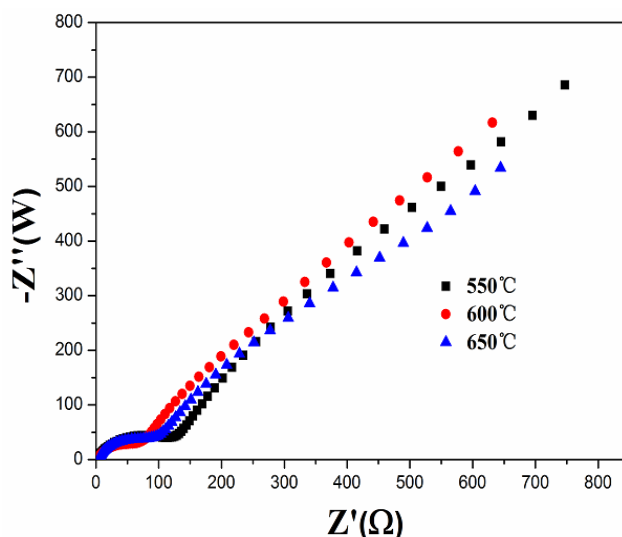


Figure 6. AC impedance diagrams of α -LiVOPO₄/C sintered at three different temperatures, after 1 cycle

To investigate whether the results of the charge transfer resistance were consistent with those of the initial capacity, EIS tests were performed. Charge transfer resistance is mainly due to the cathode impedance[35,36]. Therefore, lower electrochemical transfer resistance is more favorable for lithium insertion and disinsertion. Figure. 6 shows the impedance diagrams at different temperatures. The impedance of the materials added slightly with the added of synthesis temperature. In general, the impedance of materials was relatively small, this due to the existence of carbon layer, the electrochemical impedance for the materials was reduced. The result was consistent with the initial capacity at three temperatures.

4. CONCLUSIONS

α -LiVOPO₄/C were successfully synthesized by mechanical ball-milling method. Acetylene black was added in the synthesis process to improve the electrochemical property of the materials. Among them, LiVOPO₄/C sintered at 600 °C showed a excellent initial capacity (157.4 mAhg⁻¹) and

cycling performance after 50 cycles at 0.05 C, and with a capacity retention rate of 98.8%. In the meantime, the materials synthesized at 550 °C and 650 °C could provide the initial capacity of 150 mAh·g⁻¹ and 152.5 mAh·g⁻¹ respectively. The TEM result shows the acetylene black coating the outside surface of α-LiVOPO₄/C with the thickness of about 3.6 nm, the presence of carbon layer successfully enhanced the electrical conductivity of the material. In addition, it is significative to develop and explore these inexpensive and valid synthetic methods to provide high-performance cathode materials for mass production.

ACKNOWLEDGEMENTS

This study was supported by the Xinjiang National Natural Science Foundation of China (No:2018D01A31)

References

1. C. Delmas, M. Maccario, L. Croguennec, F. Le. Cras, F. Weill, *Nat. Mater.*, 7 (2008) 665.
2. X. Wu, L. Jiang, F. Cao, *Adv. Mater.*, 21 (2009) 2710.
3. G. Wang, H. Liu, J. Liu, *Adv. Mater.*, 22 (2010) 4944.
4. A. Boulineau, T. Gutel, *Chem Mater.*, 27 (2015) 802.
5. N. N. Bramnik, K. G. Bramnik, C. Baehtz, H. Ehrenberg, *J. Power Sources.*, 145 (2005) 74.
6. D. Wang, H. Buqa, M. Crouzet, *J. Power Sources.*, 189 (2009) 624.
7. I. Seo, B. Senthilkumar, K. H. Kim, J. K. Kim, Y. Kim, J. H. Ahn, *J. Power Sources.*, 320 (2016) 59.
8. L. Chen, B. Yan, J. Xu, Y. Chao, X. Jiang, G. Yang, *ACS Appl. Mater. Interfaces*, 7 (2015) 13934.
9. Y. Luo, X. Xu, Y. Zhang, *Adv. Energy Mater.*, 4 (2015) 1400107.
10. S. Zhu, H. Zhou, T. Miyoshi, M. Hibino I. Honma M. Ichihara, *Adv. Mater.*, 16 (2004) 2012.
11. G. Rousse, J. R. Carvajal, C. Wurm, *Chem. Mater.*, 13 (2001) 4527.
12. V. Aravindan, W. Chuiling, M. V. Redd, *Phys. Chem. Chem. Phys.*, 14 (2012) 5808.
13. V. Aravindan, W. Chuiling, S. Madhavi, *RSC Adv.*, 2 (2012) 7534.
14. K. Saravanan, H. S. Lee, M. Kuezman, *J. Mater. Chem.*, 21 (2011) 10042.
15. K. L. Harrison, C. A. Bridges, C. U. Segre, *Chem. Mater.*, 26 (2014) 3849.
16. A. S. Hameed, M. Nagarathinam, M. V. Reddy, B. V. R. Chowdari, J. J. Vittal, *J. Mater. Chem.*, 22 (2012) 7206.
17. H. Zhou, Y. Shi, F. Xin, F. Omenya, *ACS Appl. Mater. Interfaces*, 9 34 (2017) 28537.
18. N. Dupré, G. Wallez, J. Gaubicher and M. Quarton, *J. Solid State Chem.*, 177 (2004) 2896.
19. G. He, C. A. Bridges, A. Manthiram, *Chem. Mater.*, 27 (2015) 6699.
20. M. Tachez, F. Theobald and E. Bordes, *J. Solid State Chem.*, 40 (1981) 280.
21. K. H. Li, C. H. Li, C. Y. Cheng and S. L. Wang, *J. Solid State Chem.*, 95 (1991) 352.
22. J. Barker, M. Y. Saidi, J. L. Swoyer, *J. Electrochem. Soc.*, 151 (2004) A796.
23. B. L. Ellis, T. N. Ramesh, L. J. M. Davis, *Chem. Mater.*, 23 (2011) 5138.
24. C. Ling, R. Zhang and F. Mizuno, *J. Mater. Chem A.*, 2 (2014) 12330.
25. Y. Shi, H. Zhou, I.D. Seymour, *ACS Omega.*, 3 (2018) 7310.
26. Z. Liu, Z. Su and H. Tian, *Int. J. Electrochem Sci.*, 12 (2017) 10107.
27. A. Nojima, A. Sano, S. Fujita, K. Ohtsuki, S. Okada, *J. Electrochem. Soc.*, 166 (2019) A3731.
28. H. Zhou, Y. Shi, F. Xin, F. Omenya, M. S. Whittingham, *ACS Appl. Mater. Interfaces*, 9 (2017) 28537.
29. Z. Liu, Z. Su, H. Tian, *Ceram. Int.*, 44 (2018) 9372.
30. K. Cui, S. Hu, Y. Li, *Electrochim Acta*, 210 (2016) 45.

31. X. Xu, B. Dong, S. Ding, *J Math Chem.*, 2(2014) 13069.
32. A.P. Tang, Z.Q. He, J. Shen, R.X. Guo, *Adv Mater Res.*, 554 (2012) 436.
33. D.H. He, A.P. Tang, Q.W. Zhong, *Mater Sci.*, 19(2015) 423.
34. C. M. Doherty, R. A. Caruso, B. M. Smarsly, *Chem Mater.*, 21(2009) 2895.
35. H. Fang, H. Yi, C. Hu, *Electrochim Acta*, 71(2012) 266.
36. Y. B. He, M. Liu, Z. D. Huang, *J. Power Sources*, 239(2013) 269.
37. C. M. Julien, A. Mauger, K. Zaghbi, R. Veillette, H. Groult, *Ionics*, 18 (2012)625.
38. V. Aravindan, Joe Gnanaraj, Y.s. Lee, *J. Mater. Chem A.*, 1 (2013) 3518.
39. M. Zhang, N. Garcia-Araez, *J. Mater. Chem A.*, 6 (2018) 14483.
40. C. Liu, R. Massé, X. Nana, *Energy Storage Mater.*, 4 (2016) 15.

© 2021 The Authors. Published by ESG (www.electrochemsci.org). This article is an open access article distributed under the terms and conditions of the Creative Commons Attribution license (<http://creativecommons.org/licenses/by/4.0/>).